Molecular Human Reproduction, Vol.26, No.3, pp. 167–178, 2020
Advance Access Publication on January 25, 2020 doi:10.1093/molehr/gaaa009

molecular human reproduction

ORIGINAL RESEARCH

Towards uterus tissue engineering: a comparative study of sheep uterus decellularisation

T.T. Tiemann[1,2,3], A.M. Padma[1,2], E. Sehic[1,2], H. Bäckdahl[4], M. Oltean[1,5], M.J. Song[1,2,6], M. Brännström[1,2,7], and M. Hellström[1,2,*]

[1]Laboratory for Transplantation and Regenerative Medicine, Sahlgrenska Academy, University of Gothenburg, Gothenburg SE-405 30, Sweden [2]Dept. of Obstetrics and Gynecology, Sahlgrenska Academy, University of Gothenburg, Gothenburg SE-405 30, Sweden [3]Dept. of Gynecology and Obstetrics, University Hospital of Heidelberg, 69120 Heidelberg, Germany [4]Bioscience and Materials–Medical Device Technology, RISE Research Institutes of Sweden, PO Box 857, 50115 Borås, Sweden [5]Dept. of Transplantation Surgery, Sahlgrenska Academy, University of Gothenburg, Gothenburg SE-405 30 Sweden [6]Division of Gynecologic Oncology, Dept. of Obstetrics and Gynecology, Daejeon St. Mary's Hospital, The Catholic University of Korea, Seoul, South Korea [7]Stockholm IVF-EUGIN, Hammarby allé 93, 120 63 Stockholm, Sweden

*Correspondence address. Kvinnokliniken, Blå stråket 6, SE-413 45 Göteborg, Sweden. Tel: +46 721 875141; E-mail: mats.hellstrom@gu.se
https://orcid.org/0000-0003-3323-5618

Submitted on October 15, 2019; resubmitted on December 6, 2019; editorial decision on January 17, 2020

ABSTRACT: Uterus tissue engineering may dismantle limitations in current uterus transplantation protocols. A uterine biomaterial populated with patient-derived cells could potentially serve as a graft to circumvent complicated surgery of live donors, immunosuppressive medication and rejection episodes. Repeated uterine bioengineering studies on rodents have shown promising results using decellularised scaffolds to restore fertility in a partially impaired uterus and now mandate experiments on larger and more human-like animal models. The aim of the presented studies was therefore to establish adequate protocols for scaffold generation and prepare for future *in vivo* sheep uterus bioengineering experiments. Three decellularisation protocols were developed using vascular perfusion through the uterine artery of whole sheep uteri obtained from slaughterhouse material. Decellularisation solutions used were based on 0.5% sodium dodecyl sulphate (Protocol 1) or 2% sodium deoxycholate (Protocol 2) or with a sequential perfusion of 2% sodium deoxycholate and 1% Triton X-100 (Protocol 3). The scaffolds were examined by histology, extracellular matrix quantification, evaluation of mechanical properties and the ability to support foetal sheep stem cells after recellularisation. We showed that a sheep uterus can successfully be decellularised while maintaining a high integrity of the extracellular components. Uteri perfused with sodium deoxycholate (Protocol 2) were the most favourable treatment in our study based on quantifications. However, all scaffolds supported stem cells for 2 weeks *in vitro* and showed no cytotoxicity signs. Cells continued to express markers for proliferation and maintained their undifferentiated phenotype. Hence, this study reports three valuable decellularisation protocols for future *in vivo* sheep uterus bioengineering experiments.

Key words: uterus / bioengineering / decellularisation / recellularisation / foetal cells / ovine / sheep

Introduction

Novel tissue engineering techniques may be used to overcome limitations in current uterus transplantation (UTx) protocols. By using a uterus-like biomaterial that is populated with the patient's own cells, a patient-specific grafting material may instead be developed to treat uterus factor infertility. Such grafting material would not require live donor surgery or the use of immunosuppressive drugs following transplantation. Much research attention has been focused on various synthetic or biological biomaterials. A popular approach is to use decellularised tissue as scaffolding for organ and tissue reconstruction (Campo *et al.*, 2017b; Hellström *et al.*, 2017). This approach includes nuclear- and intra-cellular component removal from donated tissue. The obtained acellular organ-specific extracellular matrix (ECM) is believed to have no or very low immunogenicity and may thus serve as an excellent scaffolding for the patient-derived cells and form a patient-specific tissue or organ (Gilbert *et al.*, 2006; Badylak *et al.*, 2011). Hence, the donor material does not need tissue matching, can be harvested from any deceased donor and may therefore also provide a near-limitless supply of donor organs. These methods are continuously being optimised in animal models for a variety of tissues, e.g. heart (Ott *et al.*, 2008), liver (Shupe *et al.*, 2010; Uygun *et al.*, 2010), kidney (Song *et al.*, 2013) and reproductive organs such as the ovaries (Shea *et al.*, 2014; Laronda *et al.*, 2015; Alshaikh *et al.*, 2019) and uterus (e.g. Hellström *et al.*, 2014; Campo *et al.*, 2017a; Padma *et al.*, 2017; Campo *et al.*, 2019; Miki *et al.*, 2019). Several studies have shown that

© The Author(s) 2020. Published by Oxford University Press on behalf of the European Society of Human Reproduction and Embryology.
This is an Open Access article distributed under the terms of the Creative Commons Attribution Non-Commercial License (http://creativecommons.org/licenses/by-nc/4.0/), which permits non-commercial re-use, distribution, and reproduction in any medium, provided the original work is properly cited. For commercial re-use, please contact journals.permissions@oup.com

decellularised tissues are advantageous grafting material in a uterine wall injury model in rodents (Miyazaki and Maruyama, 2014, Santoso *et al.*, 2014; Hellström *et al.*, 2016; Hiraoka *et al.*, 2016). Specifically, these patch studies showed that fertility could be restored with bioengineered uterine grafts and that it may be a relevant treatment option for patients who have a partially impaired uterus due to e.g. malformations, extensive resection of myoma or invasive placentation. These reassuring results from experiments in small experimental animal models mandate the continuation of uterus bioengineering experiments in larger animal models. Recently, uterus decellularisation protocols were successfully optimised for larger mammals such as the rabbit (Campo *et al.*, 2019) and the pig (Campo *et al.*, 2017a). However, the sheep is by many the preferred non-primate large animal model for uterus-related studies for its close resemblance to the human in terms of the uterus size, shape, pregnancy characteristics and vascular anatomy (Dahm-Kahler *et al.*, 2008; Emmerson and Gargett, 2016; Andraus *et al.*, 2017). Preliminary results using sheep uteri proposed that SDS may be a suitable detergent for decellularisation (Daryabari *et al.*, 2019). However, the physical and bioactive properties of uterine scaffolds vary significantly due to protocol differences in scaffold generation. Differences in scaffold generation impact graft functionality *in vivo*, and it is consequently essential to evaluate this prior to any *in vivo* application. Additionally, further developments in this field may also lead to improved drug screening assays or facilitate research into fundamental biochemical events underpinning central development that may benefit from sophisticated three-dimensional *in vitro* systems that mimic normal tissue better than standard *in vitro* conditions (Olalekan *et al.*, 2017).

The aim of the present study was to establish a sound uterine biomaterial of the sheep using the decellularisation technique. Three different protocols were developed, and the resulting scaffolds were extensively examined on the basis of its ECM content, mechanistic properties and ability to support heterogeneous sheep foetal bone marrow stem cells for the recellularisation phase.

Materials and Methods

Animal work and uterus isolation

In total, 121 ovine uteri were isolated from female sheep at a local abattoir that processed animals (8–24 months old; Swedish Finull and Dutch Texel breeds) for food production. Each uterus was obtained within 5 min after an induced lethal head trauma, and the uterus was dissected free from surrounding organs on the back-table where the uterine arteries were freed and cannulated (20G, BD Neoflon, Becton Dickinson GmbH, Heidelberg, Germany). Each uterus was then perfused slowly through both arteries with ice-cold phosphate-buffered saline (PBS) including lidocaine (0.04 g/l; AstraZeneca, Gothenburg, Sweden) and heparin (5000 IU/l; Vianex S.A., Athens, Greece) until specimen blanched. Organs were kept on ice and transported to the laboratory submerged in PBS. At the laboratory, each uterus was dissected free from the surrounding tissue and frozen (−20°C) in the transport solution until further use (including all material used as control tissue). To reduce variability that could negatively affect the experiments, 32 similar-sized organs (mean = 36.42 g; ± 2.42 g SEM) were selected for the study and randomly divided into four different groups ($n = 8$), including one normal sheep uterus control group. Animal ethics approval was not needed for these experiments since all animals were killed for food production.

Decellularisation of whole sheep uterus with three different protocols

After initial technical optimisation, various decellularisation agents were evaluated on the selected thawed whole sheep uteri by placing each organ in a custom-made decellularisation perfusion set-up that was connected to silicone tubing (5-mm inner diameter; VWR, Gothenburg, Sweden) and a Masterflex perfusion pump (Cole-Parmer Instruments, Chicago, USA) that maintained a constant perfusion speed of 2–2.5 ml/min per uterine artery with a pressure that remained under 100 mmHg throughout the decellularisation procedure (Fig. 1A). All procedures were conducted at room temperature unless otherwise stated. Each uterus was first perfused with an ethylenediaminetetraacetic acid (EDTA) solution (1.86 g/l in deionised water, DW) overnight (ON) which was followed by a 2-h perfusion with DW to remove any blood remnants and cell debris after thawing. Organs were then treated with one of the following decellularisation regimens (summarised in Table I).

Protocol 1 (P1; $n = 8$): each uterus was exposed to 8-h perfusion with sodium dodecyl sulphate (SDS; 0,5% in DW) followed by DW perfusion for 26 h. The organ was then perfused with PBS overnight, then for an additional hour with Dulbecco's PBS (dPBS, Thermo Fisher, Stockholm, Sweden) at 37°C to prime the conditions for the subsequent perfusion of a recirculating DNase I solution (8000 IU DNase I/organ; D5025, Sigma Aldrich, Stockholm, Sweden) kept at 37°C for 1 h. The organ was then washed for 1 h with DW at room temperature. Immediately after the wash, a second cycle was initiated, repeating the first series of treatments starting with the SDS exposure for 8 h. After the second DNase treatment, the organ was washed for 48 h in DW, then frozen at −20°C.

Protocol 2 (P2; $n = 8$): the sequence of events was identical to those described in P1 except for the detergent. In P2, sodium deoxycholate (SDC; 2% in DW) was used instead of SDS, then each organ was frozen at −20°C.

Protocol 3 (P3; $n = 8$): a combination of two detergents; SDC (2% in DW) and Triton X-100 (1% in DW) was evaluated. The uterus was first perfused with the SDC solution for 4 h, then washed for 6 h using DW before starting the Triton X-100 perfusion for 12 h. This treatment was followed by a DW wash for 36 h, and then the whole cycle was repeated a second time. After the completion of the second cycle, a DNase I treatment was conducted in the same way as described above. Each uterus was then washed for 48 h in DW, then frozen at −20°C.

The sterilisation procedure

Each decellularised uterus was thawed and sterilised by the perfusion of peracetic acid (0.1% in a 0.9% NaCl) for 1 h. The acid was then removed, and the decellularised uterus was washed by perfusing sterile PBS for 48 h. Under aseptic conditions, multiple circular ring segments from each decellularised uterus was then evenly cut from one horn to enable biological and biophysical assessments. All tissues were then frozen in −20°C, including the excised biopsies so that assessments and quantifications would represent tissue processed in identical ways and also to enable thawing and use for potential future *in vivo* applications.

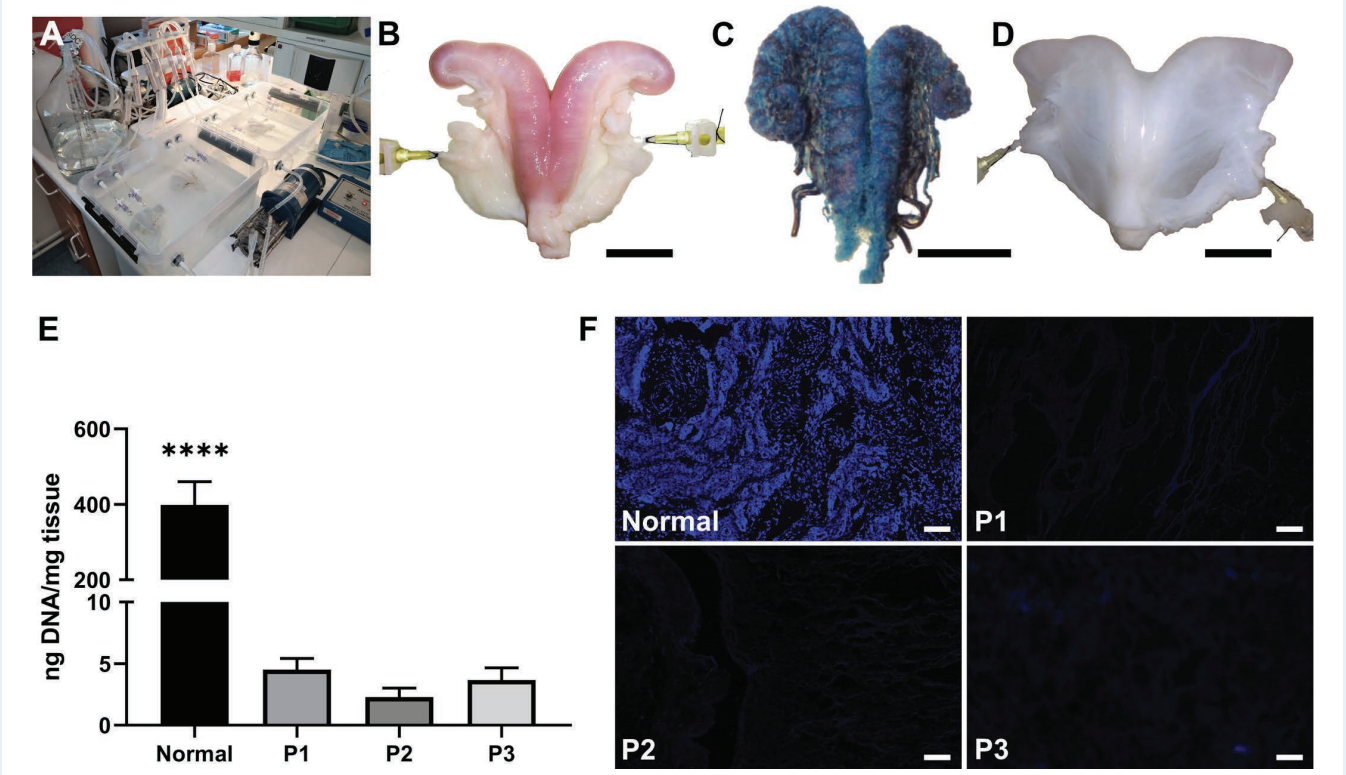

Figure 1 The sheep uterus was decellularised with three optimised protocols using a custom built perfusion system. The perfusion system (**A**) enabled four uteri to be decellularised simultaneously. Normal sheep uteri (**B**) maintained its vascular architecture after perfusion, evident by the created three-dimensional plastic model of the intact vascular network (**C**; Batson's #17 Plastic Replica Corrosion Kit; Polysciences, Eppelheim, Germany). Complete sheep uterus decellularisation (**D**) with the various decellularisation protocols was obtained in 8 days (including washing steps), and there were no apparent macroscopic differences between the protocols. DNA quantification (**E**; mean ±SEM) and DAPI-staining (**F**) confirmed effective DNA removal in all tissue layers of the uterus (DAPI images represent the myometrium-endometrium interphase). Normal, non-decellularised sheep uterus; P, protocol. Scale bars; B–D = 4 cm; F = 75 µm. Significant level = $^{****}P < 0.0001$.

Table 1 Summary of the perfusate used and the respective exposure time in the three decellularisation protocols used in the study.

Protocol 1	Protocol 2	Protocol 3
8 h SDS (0.5% in DW)	8 h SDC (2% in DW)	4 h SDC (2% in DW)
26 h DW Overnight in PBS 1 h DNase I (37°C; 8000 IU in PBS) 1 h DW Repeat once		6 h DW 12 h Triton X-100 (1% in DW) 36 h DW Repeat once 1 h DNase I (37°C; 8000 IU in PBS)
48 h DW Frozen in DW (−20°C) Thawed and sterilised with peracetic acid (1 h; 0.1% in NaCl 0.9%) 48 h sterile PBS Frozen in DW (−20°C)		

Plastic replica of the vasculature

To investigate the patency of the vasculature after uterus perfusion, Batson's plastic replica and corrosion kit was used according to the manufacturer's instructions (catalog #07349, Polysciences Europe GmbH, Eppelheim, Germany). In brief, the polymer resin was mixed and then immediately injected into respective uterine artery while the specimen was kept submerged in ice-cold water to reduce the effect from the exothermic resin reaction. The injected specimen was then

kept submerged overnight in the fridge (+4°C) and was then fully emerged in a 50°C KOH solution (20% in DW) for 24 h upon all soft tissue had dissolved and a plastic replica of the sheep uterus vasculature remained.

Histology, immunohistochemistry and electron microscopy

A thawed ring-shaped segment from each decellularised uterus was formalin-fixed and dehydrated in ethanol/xylene baths and was then paraffin-embedded before being cross-sectioned (5 µm) on a microtome. All sections were then rehydrated prior to further processing. The general morphology was investigated by light microscopy after hematoxylin and eosin (H&E) staining. The content of DNA was detected using fluorescent stain (4′,6′-diamidino-2-phenylindole, DAPI; Life Technologies, Stockholm Sweden). Standard protocols were used for Verhoeff–van Gieson (VVG) staining (to detect elastin), Masson's trichrome (MT) staining (to detect collagen) and Alcian Blue (AB) stain to detect glycosaminoglycans (GAGs; all chemicals from Histolab AB, Gothenburg, Sweden). One sample from each organ was also prepared for scanning electron microscopy (SEM) using standard procedures (conducted at the Center for Cellular Imaging, Sahlgrenska Academy, University of Gothenburg).

DNA, protein and ECM quantification

All biopsies ($n = 8$ per group and analysis) for the quantifications were thawed from −20°C and placed on dry filter paper to remove excess fluid and weighed. For DNA quantification, biopsies were independently homogenised in an ATL Buffer (including proteinase K) with a steel bead in a TissueLyser (Qiagen, Sollentuna, Sweden). Qiagen's DNA extraction kit DNeasy Blood & Tissue was used following the manufacturer's protocol. The DNA was eluded in 30 µl, and the concentration was established using a NanoDrop (Thermo Scientific, Wilmington, USA). The leftover DNA from five samples per decellularised group, including the DNA extraction from one normal uterus, was then loaded on a 2% agarose gel and run together with a DNA ladder to evaluate the size of the remaining DNA fragments in the decellularised uterine tissues.

Total protein quantification was conducted by Bradford Coomassie protein assay (#1856209; Thermo Scientific) according to standard protocols. ECM macromolecule composition of the decellularised sheep uterine tissue was evaluated using the colourimetric-based assays developed by Biocolor (Carrickfergus, UK) by following the manufacturer's instructions. To quantify soluble and insoluble collagen, the Sircol S1000 and S2000 were used, respectively. Elastin was assessed by Fastin F2000 Elastin Assay, and sGAGs were quantified using Blyscan™ B1000.

Mechanical tests

Ring-shaped biopsies (1 mm wide and containing segments of all uterine layers) from each decellularised uterus (P1, $n = 24$; P2, $n = 24$; P3, $n = 24$) were compared to control sheep uterus samples ($n = 22$). In brief, mechanical properties were evaluated with a zwickiLine testing machine (Zwick/Roell Z1.0; Zwick, Ulm, Germany). A preload of 0.1 N and a test speed of 20 mm/minute were used. The accuracy of the tensile tester was 0.5% in force and 0.5% in elongation (nominal) based on calibrations performed regularly according to ISO 7500-1:2016 and ISO 9513:2012. The maximum load, work required to completely deform the hooked tissue rings and elongation to first break were recorded. Since there was a small variability in the width between the biopsy rings, all recorded data was normalised to the width of the individual samples to exclude influence from this sampling deviation. Hence, the obtained data have the unit 'load per mm of sample width'. The selected parameters for evaluation were chosen based on the shape of the deformation diagrams.

Toxicity tests using MTT

To evaluate potential cytotoxic remnants from the decellularisation process, samples from the storage solution used for the decellularised uteri were thawed and analysed with a Cell Proliferation Kit I ($n = 6$ per protocol; #11465007001, Sigma-Aldrich) as per the manufacturer's protocol. In short, human embryonic kidney 293 cells were seeded (5000 cells) in a 96-well plate with a 100-µl standard cell culturing medium. After 24 h in culture, a 100-µl thawed storage solution from each decellularised specimen was added to a well. Some wells received 100 µl DMSO instead, which served as toxic positive control wells (for toxicity detection). Normal culturing conditions served as negative control. After 4 h, 10 µl MTT Labelling Reagent was added to each well, then the plate was incubated overnight. A kit-specific solubilisation solution was added to each well before the wells were analysed at 565 nm in a plate reader.

Sheep foetal bone marrow stem cell isolation and characterisation

A female sheep foetus, estimated to be 6–8 weeks old based on published criteria (Richardson *et al.*, 1976), was isolated from one of the pregnant uteri collected at the slaughterhouse. Unsorted, heterogeneous sheep foetal bone marrow stem cells (SF-SCs) were then isolated by flushing the femurs of the foetus with Leibovitz's L-15 Medium (Thermo Fisher) supplemented with 1% Antibiotic-Antimycotic (anti-anti; Thermo Fisher) using a 30-G needle. The cells were transferred to a cell culture flask and incubated at 37°C with air enriched with 5% CO_2 and cultured in a standard culture medium (DMEM with Glutamax, 10% foetal bovine serum and 1% anti-anti (Thermo Fisher). The female sex of the foetus was determined and confirmed by PCR on isolated genomic DNA from expanded cells using validated primers from an earlier publication (Asadpour *et al.*, 2015). To confirm the stem cellness of isolated cells and evaluate potential expression similarities with uterus cells, immunocytochemistry was conducted using antibodies from Abcam (Cambridge, UK) targeting CD166 (ab235957; 1:200), α-smooth muscle cell actin (SMA; ab32575; 1:500), vimentin (VIM; ab8978; 1:1000), Ki67 (ab15580; 1:300), oestrogen receptor-α (ER-α; ab66102; 1:100), oestrogen receptor-β1 (ER-β; ab187291; 1:100), progesterone receptor (PR; ab2765; 1:100) and cytokeratin (ab9377; 1:1000). Cells were cultured in 8-well chamber slides (Thermo Fisher), then washed with PBS and blocked for 1 h at room temperature with normal goat serum (10%) in PBS and Triton X-100 (0.2%). Antibodies were diluted in the same blocking solution and added to the cells for 1 h. Cells were then washed three times with PBS, then incubated with the appropriate fluorescent secondary antibody (CY3 or Alexa Fluor 488; Thermo Fisher; both diluted 1:300 in blocking solution). Cells were then washed again with PBS, then DAPI-treated for 1 min, then

quickly washed again in PBS before being coverslipped using fluorescent mounting media.

Recellularisation assessment

Rings of decellularised sheep uteri (0.3–0.5-mm thickness) from each protocol were recellularised using the isolated SF-SCs. The *in vitro* recellularisation experiments were carried out in triplicates and repeated three separate times ($n = 3 \times 3$; $n_{total} = 9$) for each experimental setting (Day 3 and Day 14 post recellularisation, with 1 million or 10 million cells per scaffold ring at each time point). Cells were introduced to each ring by ten separate injections using a 30-G needle (100 000 or 1 000 000 cells per injection, aimed to cover the entire ring). The experiments were terminated on Day 3 and on Day 14 after recellularisation. Each sample was fixed in a 4% buffered formaldehyde solution, then processed and embedded in paraffin for sectioning and histological analysis. Additionally, sections from each sample was rehydrated, boiled in a pressure cooker with citric acid (pH = 6.0) and then washed with PBS and stained for the same antibodies as described above.

Statistics

All statistics were performed using GraphPad Prism 8 (GraphPad, CA, USA). All the data sets were tested for normality using the Shapiro–Wilk test. When data values passed the normality test, ordinary one-way ANOVA and multiple-group comparison were used, corrected by Tukey's honest significant difference post hoc test. These data sets were plotted in bar graphs (mean ± standard error of mean, SEM) and include the graphs from the DNA quantification, total protein, GAGs, and soluble collagen, insoluble collagen and total collagen content. For data that was not normally distributed, values were presented in box plots with median and interquartile range (10–90%). The non-parametric Kruskal–Wallis test was used and Dunn's post hoc test to correct for multiple-group comparisons. Non-parametric data included the graphs for elastin and the mechanical tests.

Results

Decellularisation of whole sheep uterus with three protocols

Optimal cannulation and organ perfusion were achieved, evident by the vascular network plastic replica model of the perfused sheep uterus and the white uterus ECM structure that remained after 8 days of decellularisation procedures (Fig. 1A–D). DNA quantification and DAPI staining confirmed effective removal of nuclear material (Fig. 1E and F), and DNA significantly decreased from normal control uterus (mean value 398.4 ng/mg ± 61.4 SEM; $P < 0.0001$) to 4.5 ng/mg (±4.5 SEM; P1), 2.3 ng/mg (±2.3 SEM; P2) and 3.7 ng/mg (±3.7 SEM; P3). Electrophoresis also confirmed that only low amounts of remaining DNA were present after decellularisation, and this could only be visualised after post photo enhancement of the gel (increased contrast and brightness; Supplementary Fig. S1). This method further revealed that lingering DNA fragments were less than 500 bp in size after each decellularisation treatment.

Confirmation of morphologically preserved ECM structures

Stained normal and decellularised sheep uterus sections (Fig. 2) also revealed the removal of intracellular components. Alcian blue, which stains GAGs, showed a remaining uniformly distributed GAG content in all uterine tissue layers after decellularisation (for all protocols evaluated), suggesting a well-preserved GAG organisation. There was however a reduction in colour intensity in the processed uteri as compared to control tissue. This indicated a reduced GAG content in processed uterine tissue. Similar observations were seen after assessing VVG-stained slides that detected the elastin fibre content (black-/brown) and collagen (red). Masson's trichrome staining that identifies keratin and muscle fibres in red, and collagens in blue, indicated a substantial reduced staining intensity for keratin and muscular fibres, while collagens seemed evenly distributed following all decellularisation methods.

The ultrastructure of the decellularised tissue, imaged by SEM (Fig. 3A–H), also showed the retention of continuous ECM protein fibres, leaving a porous structure after the cells had been removed. The SDS-treated sheep uteri following P1 treatment resulted in a well-organised porous structure (Fig. 3C) while the SDC-based treatments in P2 and P3 seemed to have caused a slightly more compact scaffolding structure (Fig. 3E and G). At higher magnification, this difference was harder to identify (Fig. 3D, F and H).

Quantification of protein and ECM content, and the mechanical properties

The decellularised uterus reduced its total mean protein concentration to 7% (P1), 11% (P2) and to 6% (P3) compared with normal uterine tissue (Fig. 4A). The median elastin content was reduced to 71 and to 72% of its original content in P2 ($P = 0.024$) and P3 ($P = 0.016$), respectively. The median elastin content in P1-treated uteri was reduced to 86% of its original pretreatment content ($P = 0.351$; Fig. 4B). The sGAG content was significantly decreased to 3.2% (P1), 4.8% (P2) and 4.0% of its original content after decellularisation (Fig. 4C; $P < 0.0001$). Interestingly, the soluble collagen levels measured were not significantly different between any of the groups (Fig. 4D). However, there was a reduction in the insoluble collagen to 59% of its original content after P1 treatment ($P=0.0011$) and to 55% after P3 treatment ($P=0.0003$). Total collagen content after decellularisation followed the same pattern with a reduction to 66% after P1 ($P = 0.003$) and to 68% after P3 ($P = 0.0056$; Fig. 4E and F). Protocol 2-treated uteri did not significantly lose their insoluble or total collagen content in the process ($P = 0.0814$ and $P = 0.0507$, respectively).

Even if many of the ECM molecules were reduced by the decellularisation protocols, mechanical evaluation of circular biopsies before and after decellularisation (Fig. 5A–C) showed that the treatments made the tissue significantly stronger (maximum load; Fig. 5A; normal vs. P1, $P = 0.001$; P2, $P = 0.0332$; P3, $P < 0.0001$). However, the maximum work needed to completely destroy the decellularised tissue remained unchanged in P1- ($P = 0.0809$) and P2-treated uteri ($P = 0.0598$) and only significantly affected the tissue exposed to P3 which leads to an increased work effort ($P<0.0001$; Fig. 5B). Furthermore, the tissues' ability to extend was only significantly different for P1-treated uterine tissue ($P = 0.0069$) which increased its tissue extendibility (Fig. 5C).

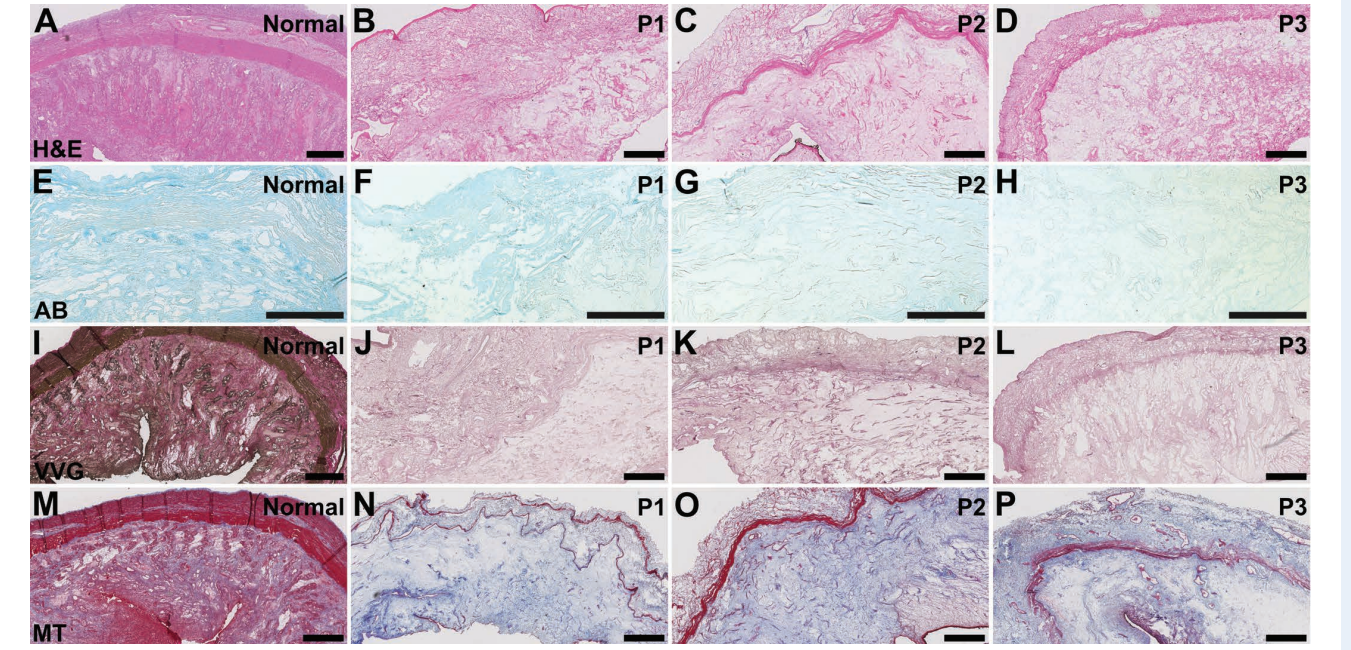

Figure 2 Histologically assessed normal and decellularised sheep uterus defined a morphologically preserved ECM using a range of different staining techniques. All hematoxylin positive cells were removed during the decellularisation process in all protocols (H&E; **A–D**). Alcian blue (AB), which stains glycosaminoglycans (GAGs), showed uniformed staining in all uterine tissue layers (**E–H**), suggesting a maintained GAGs organization. However, there was a reduction in colour intensity following decellularisation, possibly due to a reduced GAGs content. Verhoeff–van Gieson staining (VVG; **I–L** showed a reduced intensity in the elastin fibre staining (black/brown), but collagen (red) remained evenly disbursed throughout the tissue layers following decellularisation. Masson's trichrome (MT; **M–P**) staining that identify keratin and muscle fibres in red, and collagens in blue, indicated a substantial loss in keratin and muscular fibres, while collagens seemed evenly dispersed following all decellularisation methods. Normal, non-decellularised sheep uterus; P, protocol. Scale bars = 500 μm.

Hence, P2-treated uteri seemed mechanically less affected following decellularisation and were more similar to unprocessed native sheep uterus.

Cell characterisation and recellularisation *in vitro*

Cytotoxicity was not detected in any of the scaffolds using the MTT assay, suggesting that the scaffolds were free from any toxic remnants from the decellularisation process (Supplementary Fig. S2). Viable cells were observed within the scaffolds in all protocols for up to 14 days after recellularisation (Fig. 6). The cells predominantly remained in the injection site and in the superficial layers of the scaffold structures. This was independent of the initial cell density injected into the uterine scaffolds since we did not detect any obvious difference in recellularisation efficiency to constructs repopulated with 1 million cells or to those repopulated with 10 million cells (Fig. 6 and Supplementary Fig. S3). Under normal cell culturing conditions, the SF-SCs used for the recellularisation were stained positive for CD166, SMA, VIM and ER-β (Fig. 7A and E) and were negative for cytokeratin, ER-α and PR (data not shown). Many cells were also positive for the proliferation marker Ki67 (Fig. 7I). No obvious change in expression for these proteins was noticed after the cells were cultured together with the scaffolds for two weeks (Fig. 7B–D, F–H and J–L).

Discussion

This study is one of only a few that explored the principles to create bioengineered uterine tissue for the repair of surgical injuries or malformations or in the longer perspective, for donor material in a uterus transplantation. The latter procedure is now at the clinical experimental stage after proof-of-concepts demonstration of successful transplantation with live birth (Brännström *et al.*, 2015; Brännström *et al.*, 2019). This was achieved after extensive systematic animal-based research, with the sheep animal model being an important intermediate translational step from rodents to humans (Brännström *et al.*, 2012). Our new project follows the same translational approach, and we acknowledge that it will take several more years until the principle of bioengineered uterine tissue reaches the starting point for a human clinical trial. The results of the present study show how the different protocols used for the decellularisation process affect scaffold composure, specifically in regards to the collagen, elastin and sGAG content and to the mechanical properties of the scaffolds. We further show that a human-sized whole-uterus scaffold can be constructed by the three decellularisation methods presented herein.

The sheep is regarded by many as a suitable preclinical large animal model for uterus-related studies and is widely used as an experimental animal for research on reproduction. The uterus size is similar to the human uterus, as compared to the much larger, and anatomically quite

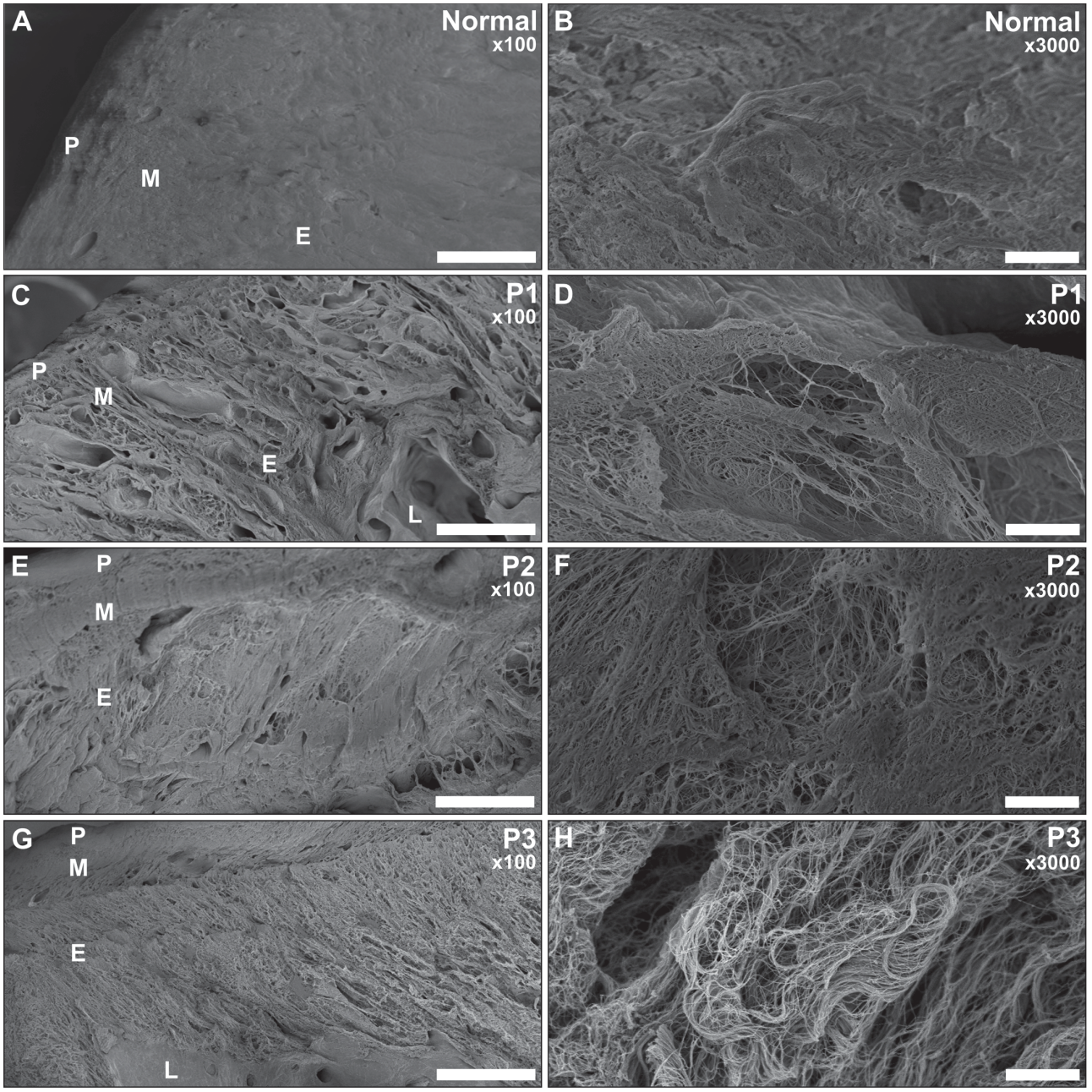

Figure 3 Scanning electron microscopy (SEM) showed a porous and fibre rich ECM after all decellularisation treatments. SEM pictures were taken at ×100 and ×3000 magnification. The SDS-treated sheep uteri following P1 resulted in a well-organised porous structure (**C**) while the SDC-based treatments in P2 and P3 seemed to have caused a more compact ECM (**E**, **G**). However, this difference was less obvious at higher magnification (**D**, **F**, **H**). P, perimetrium/protocol; M, myometrium; E, endometrium; L, lumen; Normal, non-decellularised sheep uterus. E–H represent images taken from the stroma compartment. Scale bars; SEM (×100) = 200 μm; SEM (×3000) = 5 μm.

different uteri of, for example, the pig and cow (Krause and Goh, 2009; Couri *et al.*, 2012). It has thus become the preferred non-primate large animal model for uterus transplantation practice and associated research questions (Dahm-Kahler *et al.*, 2008; Andraus *et al.*, 2017; Padma *et al.*, 2019), including uterine bioengineering (Daryabari *et al.*, 2019). Hence, novel fertility treatments using uterus bioengineering applications should be extensively optimised and evaluated on the sheep model prior to any clinical cases to study safety, graft survival and functionality.

The choice of detergents used for the decellularisation process affect the characteristics of the bioengineered construct. We therefore aimed to find various protocols that efficiently removed intracellular components while preserving the native ECM disposition, resulting in uterine scaffolds that could support added cells in the recellularisation

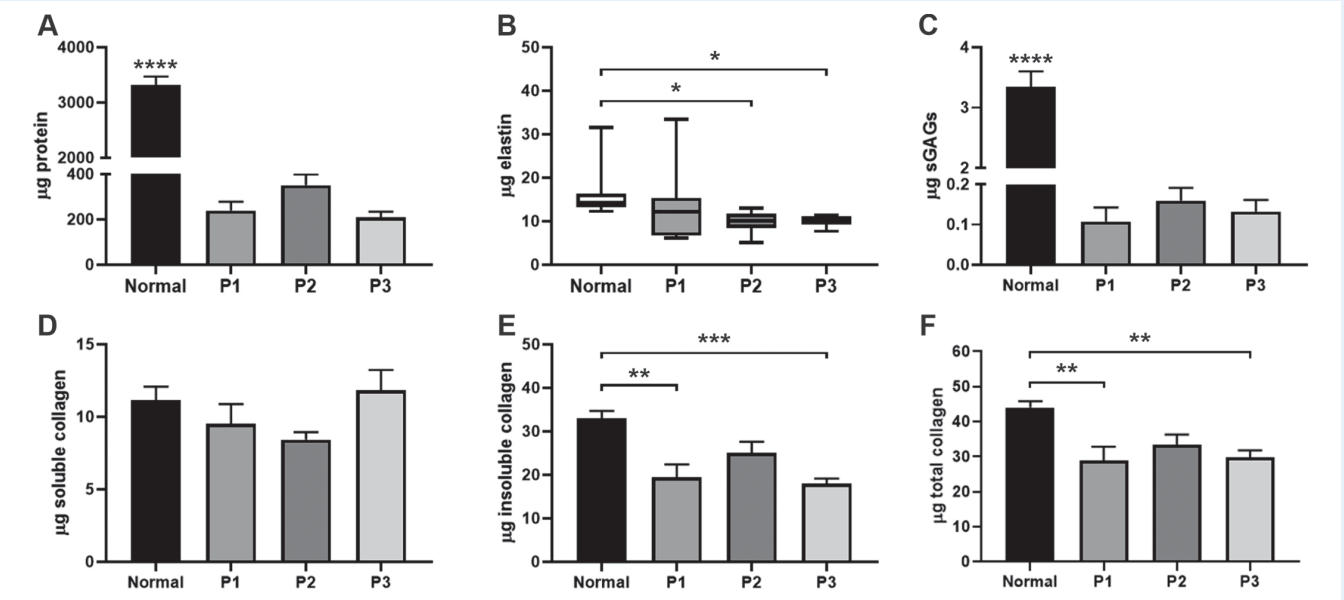

Figure 4 Decellularisation affects protein content of uterine tissue. Total protein (**A**), elastin (**B**), sulphated glycosaminoglycans (sGAGs; **C**), soluble collagen (**D**), insoluble collagen (**E**) and the total collagen (**F**) content per milligram wet tissue were quantified before and after decellularisation (bars = mean ± SEM; box plot = median ± $IQR_{10–90\%}$). The elastin content was better preserved in the SDS protocol (P1) compared to P2 and P3, but this treatment significantly removed the original insoluble collagen. Protocol 2 maintained the collagen content but significantly affected the original elastin content of the sheep uterus. Protocol 3 seemed more aggressive than the two alternative protocols since the decellularised uterine tissue in this group had significantly reduced elastin and collagen content compared to non-decellularised sheep uterus tissue.

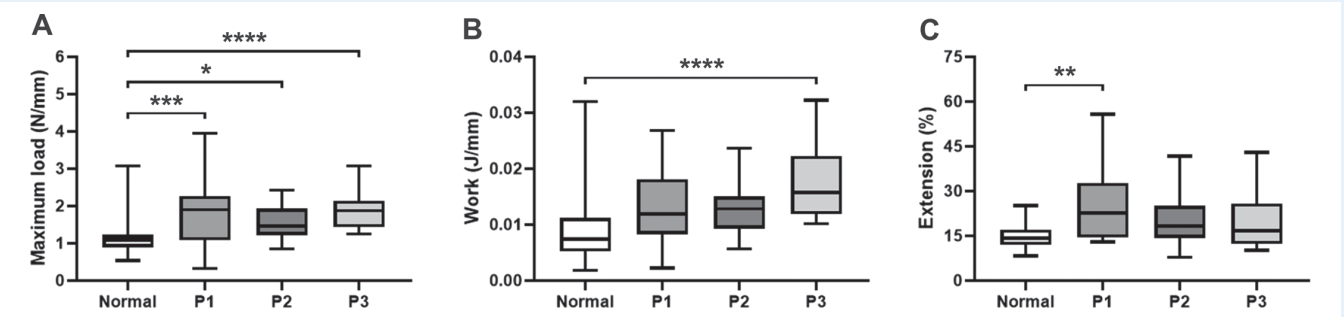

Figure 5 The mechanical properties of uterine tissues were assessed before and after decellularisation. Even if many of the ECM molecules were reduced by the decellularisation protocols, mechanical assessments of circular biopsies before and after decellularisation showed that the treatments made the tissue significantly stiffer (**A**). However, the maximum work needed to completely destroy the decellularised tissue only significantly increased in P3-treated uteri (**B**), and the tissues' ability to extend was only significantly different for P1-treated uterine tissue which led to an increased tissue extensibility (**C**). Significant levels = $^{*}P < 0.05$; $^{**}P < 0.01$; $^{***}P < 0.001$; $^{****}P < 0.0001$; see main text for the exact *P* values.

process. Our first protocol (P1) was based on 0.5% of the detergent SDS. This is a strong, effective and frequently used detergent for scaffold generation and was concluded to be the best detergent for sheep uterus decellularisation in an earlier study (Daryabari *et al.*, 2019). For the second protocol (P2), we exchanged SDS to the milder SDC detergent (2%) since we have seen some potentially negative downstream effects after the use of SDS on ovarian and blood vessel bioengineering studies (Simsa *et al.*, 2018; Alshaikh *et al.*, 2019). Our third protocol (P3) was based on a combination of the detergents SDC and Triton X-100. Triton X-100 is considered a very mild detergent and has been shown to be effective (in combination with DMSO) for the decellularisation of the much smaller rat uterus with a weight of ~1% of the sheep uterus (Hellström *et al.*, 2014; Sun *et al.*, 2016). Moreover, this Triton X-100/DMSO protocol led to better *in vivo* outcomes in the rat compared with SDS or SDC-related protocols (Miyazaki and Maruyama, 2014; Hellström *et al.*, 2016). However, we did not reach effective decellularisation during our initial experiments using Triton X-100 and DMSO for the sheep uterus, which seems to correlate to the work published by Daryabari *et al.* (2019). Instead, our three defined protocols presented herein all resulted in scaffolds containing minute donor DNA. This is essential in order to create immune system-inert scaffolds to avoid a host response and infiltration

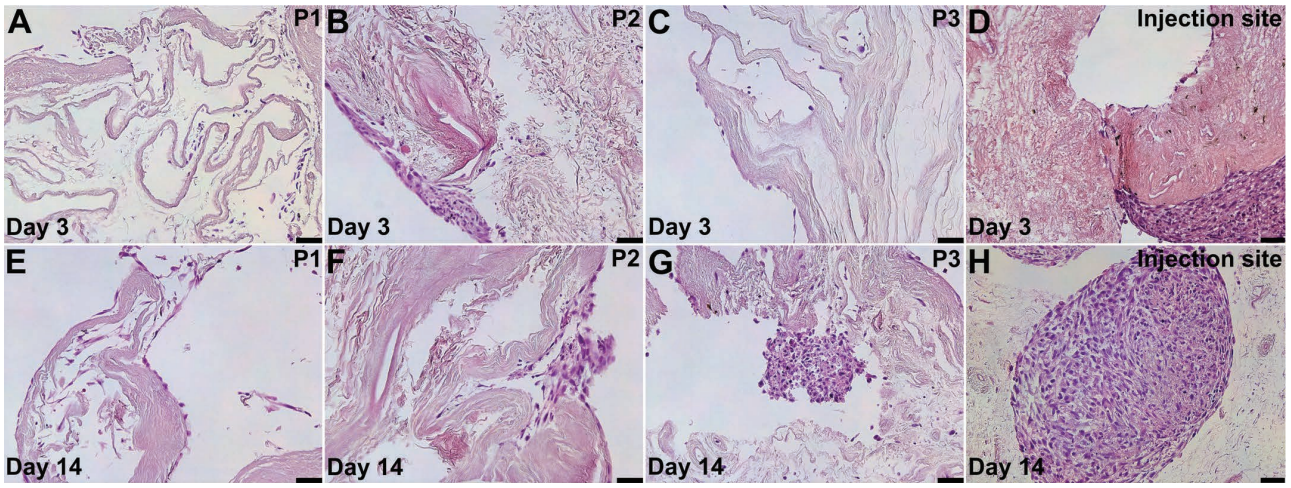

Figure 6 Hematoxylin and eosin stained sections from uterine scaffolds produced by Protocols (P) 1, 2 and 3 and recellularised with 1 million foetal sheep stem cells per scaffold ring. Cells did not migrate much from the injection sites during the two weeks assessed *in vitro* (**E–H**). On the contrary, they predominantly remained in isolated clusters within the construct or in the superficial tissue layers near the cell culturing media. Scale bars = 50 μm.

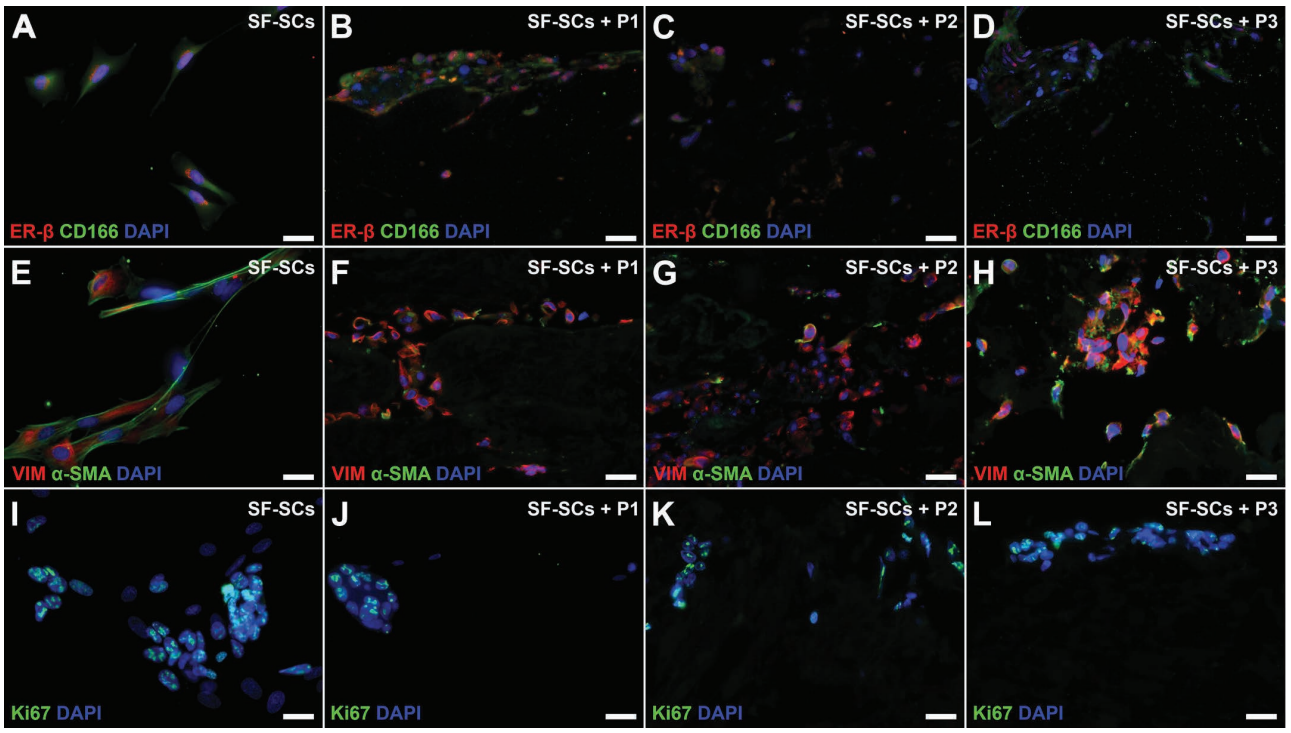

Figure 7 Cells were characterised for expression patterns after the recellularisation process. The heterogeneous sheep foetal stem cells (SF-SCs) expressed oestrogen receptor-β1 (ER-β) and CD166 (**A–D**), vimentin (VIM) and α-smooth muscle cell actin (SMA; **E–H**) and Ki67 during standard culturing conditions (**A**, E and **I**). The same expression pattern was seen after being cultured with the uterus scaffolds for 2 weeks (B–D, F–H, **J–L**). The same cells were found negative for the uterus-related proteins cytokeratin, oestrogen receptor-α and progesterone receptor (data not shown). Scale bars = 25 μm.

of inflammatory cells after engraftment (Keane *et al*., 2012; Aamodt and Grainger, 2016). Based on histology and extensive ECM quantification conducted on the three differently produced uterus scaffolds, we found that the SDS-based protocol (P1) generated scaffolds with similar elastin content compared with pretreated tissues. The sGAG content decreased significantly after all protocol treatments compared

with the normal sheep uterus tissue. This significant decrease may be explained by water solubility of sGAGs and that these molecules can be broken by the ionic detergents used in the decellularisation protocols. This reduction may however be compensated for by the addition of soluble sGAGs before recellularisation or engraftment, or by the cells themselves used for the reconstruction of the decellularised tissue (Chi Ting Au-Yeung *et al.*, 2017). Interestingly, the milder SDC-based protocol (P2) seemed better to preserve the original collagen content compared with the other protocols evaluated. Collagen is one of the major ECM components and is highly relevant for tissue regeneration and bioengineered scaffolds as it forms the base for cell attachment. Hence, P2 in this study may have an advantage over the other developed protocols. However, the scaffolding structure may also be preconditioned with collagen prior to recellularisation or engraftment to compensate for losses during the decellularisation.

Scanning electron microscopy imaging suggested that the SDS-based protocol (P1) generated a more porous acellular biomaterial compared with the other two tested protocols that featured a more dense fibre structure. Mechanically, only subtle protocol differences were observed. Scaffolds generated by P2 were more similar to native uterus tissue compared to the other structures developed. The work to fully destroy the tissue increased marginally after all decellularisation treatments, suggesting that the tissue became stronger. This may be the result of a denser ECM-fibre structure caused by the removal of cellular components. In sample preparation, we did not take into consideration whether the samples in the decellularised groups included more ECM-fibres compared with normal uterus tissue, which may happen if the decellularisation process reduced the organ size and created a denser fibre structure compared with normal tissue. However, we did not quantify any potential organ size reduction following decellularisation in these experiments, but is a point worthy to be considered in future experiments since it may impact the interpretation of the mechanical data. Nevertheless, the increased stiffness did not negatively affect the ability of the scaffold to extend before breaking, a physical attribute that may become beneficial in the event of a pregnancy after engraftment. Scaffold porosity and stiffness have long been known to play an important role in stem cell proliferation and migration (Trappmann *et al.*, 2012; Watt and Huck, 2013; Lane *et al.*, 2014) and may play a role in how added cells modulate the ECM microenvironment following recellularisation (Yue, 2014; Chi Ting Au-Yeung *et al.*, 2017).

We evaluated the ability of the scaffold to support foetal sheep stem cells *in vitro*. The recellularisation was most efficient around the injection site, in the peripheral surface area and in the inner lining on the uterine ring. The scaffold areas with limited cell population and distribution may be a consequence from a sub-optimal recellularisation technique, or perhaps deeper cell migration was limited by insufficient scaffold penetration by the culture medium. However, all scaffold types provided a vital cell culture environment for 2 weeks. Immunocytochemistry confirmed that the cells maintained the expression of proteins related to mesenchymal stem cells throughout the experiment and that the cells continued to proliferate 2 weeks after attachment to the scaffold. This indicates that the cell density within the scaffolds may improve if more time is used for the reconstruction phase. However, earlier *in vivo* rodent studies using constructs with the same limited recellularisation efficacy suggest that uterine tissue engineering strategies are effective, can stimulate regeneration and restore fertility after a severe injury to the uterine wall (Miyazaki and Maruyama, 2014; Hellström *et al.*, 2016) even without the recellularisation of decellularised tissues (Santoso *et al.*, 2014; Hiraoka *et al.*, 2016; Miki *et al.*, 2019). The cells used herein did not show any signs of differentiating into uterus-specific cell types. Thus, it may be appropriate to evaluate more uterus-like cells in future experiments for the recellularisation, e.g. autologous sheep endometrial mesenchymal stem cells (Emmerson *et al.*, 2019) or combining multiple cell types (Hellström *et al.*, 2016). However, we believe that the therapeutic effects often seen following mesenchymal stem cell transplantation can be advantageous in the initial stages following the engraftment of decellularised uterus tissue and perhaps even protect the graft from degradation when larger constructs are used (Dorin *et al.*, 2008). For these reasons, we therefore consider it useful to further optimise and improve recellularisation strategies on scaffolds used for uterus bioengineering. The cells used in the present study remained viable for up to 14 days in culture, suggesting a non-toxic scaffolding environment and therefore should also be safe to use as grafting material for future transplantation studies on the sheep model. Furthermore, recellularised constructs may also be used for preclinical three-dimensional *in vitro* experiments that better mimic the *in vivo* complexity compared to standard two-dimensional cell culturing conditions (Olalekan *et al.*, 2017). Sophisticated *in vitro* systems to explore developmental biology processes or cancer cell migration, or to study drug delivery dynamics, are warranted (Park *et al.*, 2003; Benbrook *et al.*, 2008; Sengupta *et al.*, 2008; Meng *et al.*, 2009), including *ex vivo* multi-organ test systems (Schenke-Layland and Nerem, 2011) and organs-on-chips models (Xiao *et al.*, 2017).

In summary, we present herein three promising novel sheep uterus scaffold designs that can be useful for future uterus bioengineering applications. Our research showed that an organ resembling the size of a human uterus can successfully be decellularised by using mild detergents resulting in a uterus-specific ECM scaffolding structure. Histological analysis and extensive ECM and mechanical quantifications of the decellularised tissue suggested that our SDC-protocol (P2) may be the most favourable protocol tested herein. However, the heterogeneous bone marrow-derived sheep foetal stem cells we used for recellularisation showed to be supported by all scaffolds for up to 2 weeks *in vitro*. Hence, all three developed scaffolds may prove valuable for future sheep uterus bioengineering investigations. We further addressed a major hurdle in the bioengineering field: the difficulty of establishing an efficient recellularisation across the whole scaffold. Hence, future studies will include improving the tissue reconstruction, perhaps by preconditioning with beneficial components or with improved cell application methods and/or using better cell culturing platforms that stimulate cell migration into the deeper layers of the scaffolds. Achieving an effective recellularisation will likely improve the outcomes following engraftment of a bioengineered uterine tissue and is therefore a major research topic that we intend to explore further.

Acknowledgements

The authors thank Prof. Dr J. Rom, for general guidance throughout the research phase of this publication which constitutes a major part of TTT's German doctoral thesis, and Dr Laura Carrière, for assisting with the DNA extraction, DNA quantification and electrophoresis. The authors also thank the Centre for Cellular Imaging at the University of Gothenburg and the National Microscopy Infrastructure (NMI) for providing assistance with the scanning electron microscopy.

Supplementary data

Supplementary data are available at *Molecular Human Reproduction* online.

Authors' roles

T.T.T., A.M.P. and M.J.S. conducted most of the practical work; H.B. conducted the mechanical studies; E.S. conducted the immunocytochemistry and related analysis. T.T.T., A.M.P., M.J.S., M.O., M.B. and M.H. designed the project. T.T.T., A.M.P. and M.H. drafted the manuscript. All authors contributed to the interpretation of data, conclusion regarding the results and improvements to the manuscript for its final version.

Funding

Wallenberg Research Foundation; Swedish Science Research Council (VR; 116008); Swedish state under the agreement between the Swedish government and the county council (ALF-agreement). The work was further supported by the Adlerbertska, Hjalmar Svensson and Wilhelm & Martina Lundgrens Research Foundations and a Swedish-Korean International Cooperation in Research and Higher Education (STINT) grant.

Conflict of interest

We report no conflict of interest.

References

Aamodt JM, Grainger DW. Extracellular matrix-based biomaterial scaffolds and the host response. *Biomaterials* 2016;**86**:68–82.

Alshaikh AB, Padma AM, Dehlin M, Akouri R, Song MJ, Brannstrom M, Hellstrom M. Decellularization of the mouse ovary: comparison of different scaffold generation protocols for future ovarian bioengineering. *J Ovarian Res* 2019;**12**:58.

Andraus W, Ejzenberg D, Santos RM, Mendes LR, Arantes RM, Baracat EC, D'Albuquerque LA. Sheep model for uterine transplantation: the best option before starting a human program. *Clinics (Sao Paulo)* 2017;**72**:178–182.

Asadpour R, Asadi MH, Jafari-Joozani R, Hamidian GH. Ovine fetal sex determination using circulating cell-free fetal DNA (ccffDNA) and cervical mucous secretions. *Asian Pac J Reprod* 2015;**4**:65–69.

Badylak SF, Taylor D, Uygun K. Whole-organ tissue engineering: decellularization and recellularization of three-dimensional matrix scaffolds. *Annu Rev Biomed Eng* 2011;**13**:27–53.

Benbrook DM, Lightfoot S, Ranger-Moore J, Liu T, Chengedza S, Berry WL, Dozmorov I. Gene expression analysis of biological systems driving an organotypic model of endometrial carcinogenesis and chemoprevention. *Gene Regul Syst Biol* 2008;**2**:21–42.

Brännström M, Diaz-Garcia C, Hanafy A, Olausson M, Tzakis A. Uterus transplantation: animal research and human possibilities. *Fertil Steril* 2012;**97**:1269–1276.

Brännström M, Enskog A, Kvarnström N, Ayoubi JM, Dahm-Kähler P. Global results of human uterus transplantation and strategies for pre-transplantation screening of donors. *Fertil Steril* 2019;**112**:3–10.

Brännström M, Johannesson L, Bokström H, Kvarnström N, Mölne J, Dahm-Kahler P, Enskog A, Milenkovic M, Ekberg J, Diaz-Garcia C *et al.* Livebirth after uterus transplantation. *Lancet* 2015;**385**:607–616.

Campo H, Baptista PM, Lopez-Perez N, Faus A, Cervello I, Simon C. De- and recellularization of the pig uterus: a bioengineering pilot study. *Biol Reprod* 2017a;**96**:34–45.

Campo H, Cervello I, Simon C. Bioengineering the uterus: an overview of recent advances and future perspectives in reproductive medicine. *Ann Biomed Eng* 2017b;**45**:1710–1717.

Campo H, Garcia-Dominguez X, Lopez-Martinez S, Faus A, Vicente Anton JS, Marco-Jimenez F, Cervello I. Tissue-specific decellularized endometrial substratum mimicking different physiological conditions influences in vitro embryo development in a rabbit model. *Acta Biomater* 2019;**89**:126–138.

Chi Ting Au-Yeung G, Sarig U, Sarig H, Bogireddi H, Bronshtein T, Baruch L, Spizzichino A, Bortman J, BYC F, Machluf M *et al.* Restoring the biophysical properties of decellularized patches through recellularization. *Biomater Sci* 2017;**5**:1183–1194.

Couri BM, Lenis AT, Borazjani A, Paraiso MF, Damaser MS. Animal models of female pelvic organ prolapse: lessons learned. *Expert Rev Obstet Gynecol* 2012;**7**:249–260.

Dahm-Kahler P, Wranning C, Lundmark C, Enskog A, Molne J, Marcickiewicz J, El-Akouri RR, McCracken J, Brannstrom M. Transplantation of the uterus in sheep: methodology and early reperfusion events. *J Obstet Gynaecol Res* 2008;**34**:784–793.

Daryabari SS, Kajbafzadeh AM, Fendereski K, Ghorbani F, Dehnavi M, Rostami M, Garajegayeh BA, Tavangar SM. Development of an efficient perfusion-based protocol for whole-organ decellularization of the ovine uterus as a human-sized model and in vivo application of the bioscaffolds. *J Assist Reprod Genet* 2019.

Dorin RP, Pohl HG, De Filippo RE, Yoo JJ, Atala A. Tubularized urethral replacement with unseeded matrices: what is the maximum distance for normal tissue regeneration? *World J Urol* 2008;**26**:323–326.

Emmerson S, Mukherjee S, Melendez-Munoz J, Cousins F, Edwards SL, Karjalainen P, Ng M, Tan KS, Darzi S, Bhakoo K *et al.* Composite mesh design for delivery of autologous mesenchymal stem cells influences mesh integration, exposure and biocompatibility in an ovine model of pelvic organ prolapse. *Biomaterials* 2019;**225**:119495.

Emmerson SJ, Gargett CE. Endometrial mesenchymal stem cells as a cell based therapy for pelvic organ prolapse. *World J Stem Cells* 2016;**8**:202–215.

Gilbert TW, Sellaro TL, Badylak SF. Decellularization of tissues and organs. *Biomaterials* 2006;**27**:3675–3683.

Hellström M, Bandstein S, Brännström M. Uterine tissue engineering and the future of uterus transplantation. *Ann Biomed Eng* 2017;**45**:1718–1730.

Hellström M, El-Akouri RR, Sihlbom C, Olsson BM, Lengqvist J, Bäckdahl H, Johansson BR, Olausson M, Sumitran-Holgersson S, Brännström M. Towards the development of a bioengineered uterus: comparison of different protocols for rat uterus decellularization. *Acta Biomater* 2014;**10**:5034–5042.

Hellström M, Moreno-Moya JM, Bandstein S, Bom E, Akouri RR, Miyazaki K, Maruyama T, Brännström M. Bioengineered uterine

tissue supports pregnancy in a rat model. *Fertil Steril* 2016;**106**:487, e481–496.

Hiraoka T, Hirota Y, Saito-Fujita T, Matsuo M, Egashira M, Matsumoto L, Haraguchi H, Dey SK, Furukawa KS, Fujii T *et al*. STAT3 accelerates uterine epithelial regeneration in a mouse model of decellularized uterine matrix transplantation. *JCI insight* 2016;**1**.

Keane TJ, Londono R, Turner NJ, Badylak SF. Consequences of ineffective decellularization of biologic scaffolds on the host response. *Biomaterials* 2012;**33**:1771–1781.

Krause H, Goh J. Sheep and rabbit genital tracts and abdominal wall as an implantation model for the study of surgical mesh. *J Obstet Gynaecol Res* 2009;**35**:219–224.

Lane SW, Williams DA, Watt FM. Modulating the stem cell niche for tissue regeneration. *Nat Biotechnol* 2014;**32**:795–803.

Laronda MM, Jakus AE, Whelan KA, Wertheim JA, Shah RN, Woodruff TK. Initiation of puberty in mice following decellularized ovary transplant. *Biomaterials* 2015;**50**:20–29.

Meng CX, Andersson KL, Bentin-Ley U, Gemzell-Danielsson K, Lalitkumar PG. Effect of levonorgestrel and mifepristone on endometrial receptivity markers in a three-dimensional human endometrial cell culture model. *Fertil Steril* 2009;**91**:256–264.

Miki F, Maruyama T, Miyazaki K, Takao T, Yoshimasa Y, Katakura S, Hihara H, Uchida S, Masuda H, Uchida H *et al*. The orientation of a decellularized uterine scaffold determines the tissue topology and architecture of the regenerated uterus in ratsdagger. *Biol Reprod* 2019;**100**:1215–1227.

Miyazaki K, Maruyama T. Partial regeneration and reconstruction of the rat uterus through recellularization of a decellularized uterine matrix. *Biomaterials* 2014;**35**:8791–8800.

Olalekan SA, Burdette JE, Getsios S, Woodruff TK, Kim JJ. Development of a novel human recellularized endometrium that responds to a 28 day hormone treatment. *Biol Reprod* 2017.

Ott HC, Matthiesen TS, Goh SK, Black LD, Kren SM, Netoff TI, Taylor DA. Perfusion-decellularized matrix: using nature's platform to engineer a bioartificial heart. *Nat Med* 2008;**14**:213–221.

Padma AM, Tiemann TT, Alshaikh AB, Akouri R, Song MJ, Hellstrom M. Protocols for rat uterus isolation and decellularization: applications for uterus tissue engineering and 3D cell culturing. *Methods Mol Biol* 2017.

Padma AM, Truong M, Jar-Allah T, Song MJ, Oltean M, Brannstrom M, Hellstrom M. The development of an extended normothermic ex vivo reperfusion model of the sheep uterus to evaluate organ quality after cold ischemia in relation to uterus transplantation. *Acta Obstet Gynecol Scand* 2019.

Park DW, Choi DS, Ryu HS, Kwon HC, Joo H, Min CK. A well-defined in vitro three-dimensional culture of human endometrium and its applicability to endometrial cancer invasion. *Cancer Lett* 2003;**195**:185–192.

Richardson C, Hebert CN, Terlecki S. Estimation of the developmental age of the ovine fetus and lamb. *Vet Rec* 1976;**99**:22–26.

Santoso EG, Yoshida K, Hirota Y, Aizawa M, Yoshino O, Kishida A, Osuga Y, Saito S, Ushida T, Furukawa KS. Application of detergents or high hydrostatic pressure as decellularization processes in uterine tissues and their subsequent effects on in vivo uterine regeneration in murine models. *PloS one* 2014;**9**:e103201.

Schenke-Layland K, Nerem RM. In vitro human tissue models–moving towards personalized regenerative medicine. *Adv Drug Deliv Rev* 2011;**63**:195–196.

Sengupta S, Sengupta J, Mittal S, Kumar S, Ghoshi D. Effect of human chorionic gonadotropin (hCG) on expression of vascular endothelial growth factor a (VEGF-a) in human mid-secretory endometrial cells in three-dimensional primary culture. *Indian J Physiol Pharmacol* 2008;**52**:19–30.

Shea LD, Woodruff TK, Shikanov A. Bioengineering the ovarian follicle microenvironment. *Annu Rev Biomed Eng* 2014;**16**:29–52.

Shupe T, Williams M, Brown A, Willenberg B, Petersen BE. Method for the decellularization of intact rat liver. *Organogenesis* 2010;**6**:134–136.

Simsa R, Padma AM, Heher P, Hellstrom M, Teuschl A, Jenndahl L, Bergh N, Fogelstrand P. Systematic in vitro comparison of decellularization protocols for blood vessels. *PloS One* 2018;**13**:e0209269.

Song JJ, Guyette JP, Gilpin SE, Gonzalez G, Vacanti JP, Ott HC. Regeneration and experimental orthotopic transplantation of a bioengineered kidney. *Nat Med* 2013;**19**:646–651.

Sun J, Zhang X, Cao Y, Zhao Q, Bao E, Lv Y. Ovarian toxicity in female rats after oral administration of melamine or melamine and cyanuric acid. *PloS one* 2016;**11**:e0149063.

Trappmann B, Gautrot JE, Connelly JT, Strange DG, Li Y, Oyen ML, Cohen Stuart MA, Boehm H, Li B, Vogel V *et al*. Extracellular-matrix tethering regulates stem-cell fate. *Nat Mater* 2012;**11**:642–649.

Uygun BE, Soto-Gutierrez A, Yagi H, Izamis ML, Guzzardi MA, Shulman C, Milwid J, Kobayashi N, Tilles A, Berthiaume F *et al*. Organ reengineering through development of a transplantable recellularized liver graft using decellularized liver matrix. *Nat Med* 2010;**16**:814–820.

Watt FM, Huck WT. Role of the extracellular matrix in regulating stem cell fate. *Nat Rev Mol Cell Biol* 2013;**14**:467–473.

Xiao S, Coppeta JR, Rogers HB, Isenberg BC, Zhu J, Olalekan SA, McKinnon KE, Dokic D, Rashedi AS, Haisenleder DJ *et al*. A microfluidic culture model of the human reproductive tract and 28-day menstrual cycle. *Nat Commun* 2017;**8**:14584.

Yue B. Biology of the extracellular matrix: an overview. *J Glaucoma* 2014;**23**:S20–S23.